A crop-specific and time-variant spatial framework to characterize production environments: A case study for rainfed wheat in Ethiopia

Habtamu S. Gelagay [abc*], Louise Leroux[abc], Lulseged Tamene[d], Meklit Chernet[e], Gerald Blasch[f], Degifie Tibebe[d], Wuletawu Abera[d], Tesfaye Sida[f], Kindie Tesfaye [fg], Marc Corbeels[abc], João Vasco Silva [h]

[a]AIDA, University of Montpellier, CIRAD, Montpellier, France

[b]CIRAD, UPR AIDA, Nairobi, Kenya

[c] International Institute of Tropical Agriculture(IITA), Nairobi, Kenya

[d]International Center for Tropical Agriculture (CIAT), Addis Ababa, Ethiopia

[g] Alliance for a Green Revolution in Africa (AGRA), Nairobi, Kenya

[e] The Alliance of CIAT and Bioversity,Rome, Italy

[f]International Maize and Wheat Improvement Center (CIMMYT), Addis Ababa, Ethiopia

[h]International Maize and Wheat Improvement Center (CIMMYT), Zimbabwe, Harare

[*]Corresponding author: Habtamu Sewnet Gelagay, habtamu_sewnet.gelagay@cirad.fr

Abstract

1. CONTEXT

Addressing the limitations of scaling agronomic recommendations, which are usually confined to small areas, requires a spatial framework for characterizing production environments in a timely and cost-effective manner.

2. OBJECTIVE

This study aimed to introduce a data-driven framework to characterize rainfed wheat crop production

environments in Ethiopia. The framework entails mapping of the annual rainfed wheat area and the delineation of crop-specific and dynamic agro-ecological spatial units (ASUs).

3. METHODS

An ensemble machine learning approach built upon time-series satellite images and environmental data was used for crop type mapping while pixel- and object-based clustering algorithms were used to delineate dynamicASUs from two temporal perspectives: annual ASUs for the 2021 and 2022 growing seasons to assess short-term dynamism, and ASUs from aggregated data (2016 - 2022) to capture long-term variations in the production environment.

4. RESULTS AND CONCLUSIONS

Model evaluation showed that the ensemble of random forest, gradient boosting, and classification and regression trees predicted wheat cropland in the 2021 and 2022 growing seasons with 88-90% accuracy. A concordance in defining ASUs between pixel- and object-based approaches was observed with consistency and dynamism in ASUs from 2021 to 2022 and between single-year and aggregated ASUs across approaches. This consistency and dynamism in ASUs highlight the spatial scalability and temporal flexibility of the framework, which allows for characterizing production environments across scales and analyzing trends and fluctuations, providing valuable insights for addressing food security and environmental challenges.

5. SIGNIFICANCE

The developed spatial framework could facilitate future yield gap analysis and agronomic assessments for rainfed wheat in Ethiopia and be transfered to other crops and production environments.

Keywords: Crop type mapping, spatial unit zonation, Yield Gap, Google Earth Engine, multi-source remote sensing

1. Introduction

Characterization of production environments on a large scale is essential for targeted interventions, informed decision-making, and a sustainable solution for global food security (Cassman and Grassini, 2020). Yet, the scope of agronomic information derived from on-farm trials, field experiments and crop model simulations is mostly limited to small areas due to the high cost and time required to obtain the necessary input data (Ramirez-Villegas and Challinor, 2012; van Bussel et al., 2015; Beza et al., 2017) and the need to account for biophysical variability across different agricultural landscapes (Veldkamp et al., 2001). There are also challenges in capturing temporal variability in the production environment over different growing seasons. A spatial framework that can account for spatio temporal variability a corss cropland cohorts sharing similar biophysical attributes is essential to scaling out agronomic research for development efforts.

A prominent spatial framework to characterize crop production environments is the climatic zonation scheme of the Global Yield Gap Atlas (GYGA-CZ; van Wart et al., 2013). Other examples include the Technology Extrapolation Domain (TED) framework (Edreira et al., 2018) and the Similar Response Unit

(SRU) framework (Tamene et al., 2022). However, most past efforts remain too coarse, generic, and static for technology targeting in complex production landscapes and often involve subjective decisions when segmenting environments based on a limited number of variables. For instance, the GYGA-CZ focused on three climatic variables, overlooking important variation in edaphic factors and landscape characteristics inherent to smallholder production systems of sub-Saharan Africa (Vanlauwe et al., 2007; Amede et al., 2022). Moreover, existing frameworks are crop-agnostic, hence not able to inform targeting of crop-specific interventions and responses to environmental conditions (Porter and Semenov, 2005), and rely on expert opinion-driven matrix zonation, introducing subjectivity and limiting transferability across landscapes (Williams et al., 2008). They are also static and not able to capture inter- and intra-annual variation in environmental conditions, a key feature of rainfed crop production systems. Such limitations translate into products that are often too coarse and generic to guide research and development activities at the local level.

Crop production in sub-Saharan Africa takes place in smallholder production systems characterized by small and fragmented farms (Giller et al., 2021; Headey et al., 2014; Fritz et al., 2015) and heterogeneous landscapes (Kassawmar et al., 2018; Tamene et al., 2022). Shifts in cultivated areas are also common over time (Bussel et al., 2015). Spatial frameworks for characterizing production environments in such contexts thus need to rely on up-to-date and fine-scale crop area distribution data (See et al., 2015; Bussel et al., 2015) and crop-specific and dynamic agro-ecological zonation schemes that can capture variations in the production environment. Given the diverse thermal, moisture, soil, and terrain requirements of different crops (You et al., 2009), data-driven spatial frameworks built upon multi-source and multi-thematic data can assist in the near real-time delineation of crop-specific agro-ecological spatial units (ASUs) that maximize the within-zone homogeneity while minimizing the number of zones required to cover a specific crop area.

The objective of this study was to introduce and operationalize a crop-specific and dynamic spatial framework for segmenting and characterizing heterogeneous and diverse crop production environments. The framework entails the prediction of crop area distribution and the delineation of ASUs through integrating high-resolution Earth Observation (EO) data and environmental data with ground observations. ASUs refer to homogeneous spatial units sharing similar biophysical conditions in which crop production technologies are likely to perform similarly. We assumed that (1) delineating the target crop type distribution area is required for crop-specific zonation to strike a balance between within-unit variability and the number of units required to cover the targeted crop areas, and (2) dynamic ASUs can capture time variant characteristics of rainfed crop production systems. This effort can benefit from the availability of high spatial and temporal resolution, as well as spectrally rich satellite images (e.g., Sentinel-1 and Sentinel-2) and accessible cloud computing platforms such as Google Earth Engine.

The proof of concept of our spatial framework was conducted for smallholder wheat production systems in Ethiopia. Wheat is of strategic importance to national food security in the country due to high import dependency (Silva et al., 2023, Tadesse et al., 2022; Senbeta and Worku, 2023). The crop is predominantly cultivated under rainfed conditions on fertile, loamy, black soils with high water-holding capacity (Falco et al., 2005), in highlands and mid-altitudes areas during the main rainy season spanning between June and November (White et al., 2001; Mersha, 2000). Technology targeting in the complex wheat production landscapes of Ethiopia can guide investments aiming to increase wheat productivity and resource-use efficiency in farmers' fields, which remain well below what is biophysically possible with improved agronomic practices (Silva et al., 2021). For this reason, the relevance of the newly introduced framework is discussed in the context of technology targeting in support of national food security and yield gap analysis. Yet, its applicability can be extended to other crops and production environments in a cost-effective way.

2. Materials and Methods

2.1. Methodological approach

A spatial framework integrating the broader agroecological context of the Ethiopian wheat belt was developed and operationalized in Google Earth Engine (Gorelick et al., 2017). The Ethiopian wheat belt denotes the cropland and non-cropland areas suitable for cultivation of rainfed wheat and of other similar crop types (Tadesse et al., 2022). Our data-driven framework comprises two-steps (Figure 2): (1) mapping the annual rainfed wheat areas for the 2021 and 2022 Meher growing seasons and (2) developing dynamic ASUs within the Ethiopian rainfed wheat belt to characterize the agro-ecological conditions under which wheat production takes place.

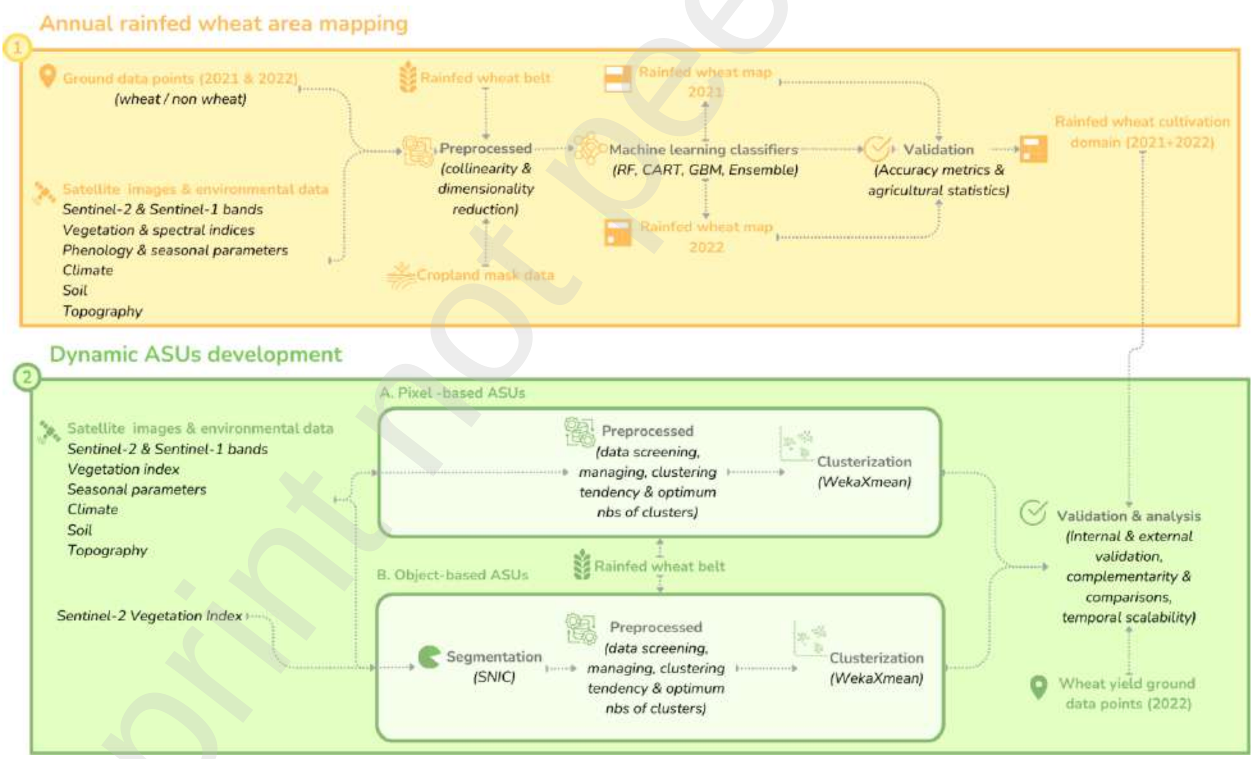

Figure 1 | Two step data-driven spatial framework to map cropland area and delineate agro-ecological spatial units (ASUs) based on the integration of multi-source time series satellite images and environmental data. Step 1 entails the spatial prediction of the annual rainfed wheat area. Step 2 entails the delineation of crop specific and dynamic ASUs with two complementary approaches, pixel- and object-based clustering. RF stands for Random Forest, CART for Classification and Regression Tree, GBM for Gradient Boosting Machine and SNIC for Simple Non-Iterative Clustering.

2.2. Rainfed wheat area mapping

Crop-type field data were collected during the 2021 and 2022 Meher growing seasons to train and evaluate models for rainfed wheat area mapping. A total of 1651 (1251 wheat fields and 400 fields of other crops) and 2927 (1747 wheat fields and 1180 fields of other crops) ground truth points were inventoried in 2021 and 2022, respectively. To ensure a balanced representation between wheat and other crops in the data sets and to reduce bias and model inaccuracy caused by class imbalance, additional ground truth points representing non-wheat areas were generated using a decision rule approach (Ghazaryan et al., 2018) for the 2021 Meher growing season. To that end, the composite Normalized Difference Vegetation Index (NDVI) (mean and maximum) and seasonal information (phase and amplitude) from Sentinel-2 NDVI data were extracted for all wheat ground truth points. Subsequently, criteria for wheat-specific characteristics, such as NDVI mean (0.53 to 0.6), peak (0.7 to 0.8), phase (0.35 to 0.56), and amplitude (0.5 to 1), were used as decision rules for discriminating between wheat and non-wheat points. Following this, 1000 random points were extracted from the 10-meter Digital Earth Africa cropland dataset (DEA, 2021), and the composite NDVI and seasonal information were extracted as for the wheat ground truth points. Random points with values within the specified wheat characteristics were removed, resulting in the identification of 516 non-wheat points.

Sentinel-1 and Sentinel-2 satellite images and derived variables were integrated with a variety of environmental data to predict the rainfed wheat area distribution (Figure 1; Table S1). Time series information including spectral bands, vegetation indices (e.g., NDVI), and spectral indices (e.g., greenness index) derived from Sentinel-2 satellite images, and backscatter coefficients derived from Sentinel-1 satellite images between mid-June to late November, coinciding with the critical growth phases of rainfed wheat crops in Ethiopia, were considered. The fusion of Sentinel-1 and Sentinel-2 satellite images allows to address temporal gaps due to cloud cover in Sentinel-2 satellite images, thus facilitating the discrimination of wheat crop growth stages from those of other similar crop types (Ofori-Ampofo et al., 2021). Phenological information, determined by a 20% threshold for season start and 50% for season end, along with seasonal information, were derived from Sentinel-2 NDVI time series using the threshold approach for phenology (Jonsson and Eklundh, 2002) and harmonic transformation for seasonal parameters (Jakubauskas et al., 2001). This information allowed us to capture the different wheat growth stages (Lu et al., 2014) and the cyclical patterns (repetitive fluctuation) of environmental variables affecting wheat development (Ghazaryan et al., 2018; Jakubauskas et al., 2002). Climatic (mean monthly precipitation, temperature, and solar radiation), topsoil (organic carbon, pH, and texture), and topographic (elevation and slope) factors were also included as predictors to account for spatial variations in wheat crop phenology influenced by agro-ecological gradients (Blickensdörfer et al., 2022; Wang et al., 2019). All predictors were masked to the crop land mask (Zanaga et al.,2022) within the rainfed wheat belt (Supplementary Figure S1) prior to the model fitting.

An ensemble of three machine learning algorithms commonly used for land cover and land use mapping (e.g., Bui et al., 2021; Li et al., 2023; Xu et al., 2018) were used to predict the wheat area distribution for the 2021 and 2022 Meher growing seasons. The models were fitted per growing season considering 70% of the ground truth points for model training and the remaining 30% for model evaluation. The machine learning algorithms included random forest (RF; Breiman, 2001), classification and regression tree (CART; Breiman et al., 1984), and gradient boosting (GB; Friedman, 2001). Results from the three algorithms were ensembled using a majority voting approach (Ahmed et al., 2023) in which grid cells classified as wheat by two or three algorithms were combined, resulting in a final ensemble wheat distribution map. The predicted wheat area distribution for the two growing seasons were then merged to capture general geographical patterns and trends in wheat cultivation over time in Ethiopia.

2.3. Delineation of dynamic ASUs

A data-driven approach was adopted to delineate dynamic ASUs (Figure 1). Two analytical approaches were employed to understand the short-term variation and longer-term trends in ASUs. First, we established two sets of ASUs for the 2021 and 2022 growing seasons using year-specific features (Supplementary Table S1) which captured short-term variations in ASUs. Second, ASUs were developed using aggregated features over a period of seven years (2016–2022) to capture longer-term trends in the production environment.

ASUs zonation relied on climatic, soil, topographic, and remote sensing data known to influence crop growth and development (Supplementary Table S1). Climatic variables included growing degree days (GDD), temperature seasonality, and aridity index as monthly averages over the growing season (see also van Wart et al., 2013). GDD was calculated by subtracting the mean monthly temperatures, derived from Muñoz Sabater (2019), from the wheat's base temperature of 2 ^{o}C (Simane, 1999). Temperature seasonality was calculated as the standard deviation of the monthly average temperature derived from Abatzoglou et al. (2018). The aridity index was calculated as the ratio of annual total precipitation (Funk et al., 2015) to total potential evapotranspiration (Trabucco and Zomer, 2018). Soil variables and topographic factors were included in the zonation scheme because climatically suitable zones may lack the necessary soil and topographic attributes for rainfed wheat cultivation. Soil predictors included pH, organic carbon, and texture class (Hengl et al., 2021), and plant available water holding capacity estimated with the texture class-based estimation method (Grossman and Reinsch, 2002). Topographic features included elevation and slope (Farr et al., 2007). Remote sensing variables, including vegetation indices, synthetic aperture radar (SAR) backscatter, and seasonal information, were considered to capture the spatiotemporal variability in vegetation, thereby supporting a dynamic ASU zonation.

We adopted a clustering approach for ASUs development, leveraging its capacity to handle multiple input variables, minimize intraclass variability, and mitigate subjectivity in class definition. This approach relies on measuring similarity using distance functions, where smaller distances indicate higher similarity within units (Cao et al., 2012; Xu and Wunsch, 2005). Two clustering approaches were employed. The pixel-based approach clusters individual grid cells based on their intrinsic values, hence capturing fine spatial patterns which are important for agronomic assessments at local level. Conversely, the object-based approach involves generating super-pixels, extracting their mean feature values, and clustering the extracted means. This approach thus allows the generalization of complex patterns, making it suitable for agronomic assessments across large scales.

For pixel-based clustering, the variables presented in Supplementary Table S1 were extracted for the rainfed wheat belt (Supplementary Figure S1), followed by preprocessing and feature engineering with rescaling, normalization, multicollinearity analysis, and dimensionality reduction. Secondly, the proximity distance (Puzicha et al., 2000; Green and Rao, 1969) between variables was examined to gain insights into the data's internal structure. Thirdly, the optimum number of clusters (referred to as ASUs in this context) was defined based on the elbow method (Kwedlo, 2011), the silhouette coefficient (Kaufman and Rousseeuw, 2009; Rousseeuw, 1987), and the Bayesian Information Criterion (BIC, Fraley and Raftery, 1998; Neath and Cavanaugh, 2012). The elbow method minimizes the total within-cluster sum of squares (WSS), and the point at which the graph forms an elbow indicates the optimal cluster count (Brock et al., 2008). The silhouette coefficient gauges cluster quality by assessing data cohesion within clusters and inter-cluster separability, with a higher average silhouette width indicating better clustering (Tomasini et al., 2016). BIC balances the goodness-of-fit and model complexity, with the lowest value indicating the optimal number of clusters (Fraley and Raftery, 1998; Gao, 2010; Jones, 2011). Finally, pixel-based clustering was conducted with the WekaXmean clustering algorithm (Beckham et al., 2016; Arthur and Vassilvitskii, 2007), an extension of k-means clustering (Pelleg and Moore, 2000) in Google Earth Engine

For object-based clustering, the initial step involved super-pixel segmentation of a time series of Sentinel-2 NDVI data spanning between 2016 and 2022. This segmentation was achieved through the application of the Simple Non-Iterative Clustering (SNIC) algorithm, an advanced variant of Simple Linear Iterative Clustering (SLIC; Mi and Chen, 2020). Super-pixel segmentation aims to create coherent grid cell groupings (Stutz et al., 2018), serving as objects for feature extraction in subsequent steps. This grouping of grid cells into super-pixels aims to capture higher-level information from satellite images by analyzing these objects as units rather than isolated grid cells. The mean values of the features used in pixel-based ASUs (see Supplementary Table S1) were then extracted within each super-pixel. An analogous procedure and algorithmic approach to that used for pixel-based clustering was then applied to establish the object-based ASUs.

The optimum number of ASUs were numerically labeled and are conditional on the clustering approach and data aggregation procedure. Thus, they may not represent the same spatial extent for two different clustering approaches. The evaluation and comparison of the two approaches, pixel and object, is explained in Section 2.4.

2.4. Evaluation of model performance and analysis of ASUs

The accuracy of the rainfed wheat distribution maps generated by each algorithm and their ensemble was assessed using the overall accuracy (OA), the kappa index, and the producer accuracy (PA) and user accuracy (UA). Each algorithm's ability to generalize unseen data from different time periods was also evaluated. For instance, the three algorithms were trained using data from the 2021 Meher growing season and evaluated on unseen data from 2022 Meher growing season, and vice versa. National statistics on rainfed wheat harvested area (CSA, 2022; FAOSTAT, 2022) were also used to evaluate the crop area estimated with our approach against official statistics at regional and national levels.

The validity and practical significance of both pixel- and object-based ASUs derived from features aggregated over the period 2016–2022 were tested using internal and external evaluation metrics. Internal evaluation included assessing between-unit separability using Kruskal-Wallis tests (Kruskal and Wallis, 1952) for selected input variables (Supplementary Table S1) and silhouette coefficients (Tomasini et al., 2016) to check within-unit cohesion and between-unit separability. External evaluation of ASUs relied on wheat yield data collected with crop cuts (n=1560) during the 2022 Meher growing season as external information, and a Kruskal-Wallis test was conducted using these data to assess statistically significant differences in wheat yield across ASUs.

The similarity between pixel-and object-based ASUs, as well as the temporal scalability and dynamism of ASUs over time, were evaluated using proximity analysis (Puzicha et al., 2000) through pairwise distance measurements. The comparison between pixel- and object-based ASUs aimed to determine the similarity between pixel- and object-based ASUs, serving as a means of evaluating the accuracy and reliability of each approach and the extent they can capture similar spatial patterns in ASU delineation. Temporal scalability and dynamism aimed to evaluate whether ASUs could capture changes in the production environment over time. In this regard, we examined the stability and variation between ASUs derived from the single-year (2021 and 2022) and aggregated (2016–2022) datasets for both pixel- and object-based clustering. ASUs from single-year datasets were referred to as 'single-year ASUs', and ASUs developed from the 2022 dataset were used as examples of this type, while those from multi-year datasets (2016–2022) were labeled 'aggregate ASUs'. The distinction between single-year and aggregate ASUs enabled us to examine the dynamics of the delineated ASUs over time. The ASUs generated with the pixel- and object-based approaches were then masked to the spatial extent of the rainfed wheat area predicted for Ethiopia (Section 2.2). Subsequently, cumulative probability distribution functions were developed to assess the distribution and changes of ASUs across the rainfed wheat belt and the rainfed wheat area over time in both clustering approaches.

3. Results

3.1 Rainfed wheat area in Ethiopia

A distinct geographical pattern in the distribution of rainfed wheat areas, concentrated in the central region and expanding to the northern parts of Ethiopia, was evident in both growing seasons (Figures 3). The three algorithms reached high classification accuracies in the two growing seasons (OA > 90% and Kappa > 0.85), with the highest accuracy reported for gradient boosting in the 2022 growing season (OA = 97% and Kappa = 0.92; Supplementary Table S2). An OA of 88% for the 2021 growing season and 94% for the 2022 growing season was reported for the ensemble model (Supplementary Table S2). The algorithms also performed well in identifying wheat areas, with user accuracy of 92-96% and producer accuracy of 95-97%. The ensemble model generalizability assessment was achieved with an OA of 70% when trained on the 2021 data and tested on the 2022 data and an OA of 90% when trained on the 2022 data and tested on the 2021 data, hence being able to generalize unseen data from different growing seasons (Supplementary Table S2). Elevation, solar radiation, and precipitation were the most important features to map the rainfed wheat cropland in Ethiopia (Supplementary Figure S2).

The rainfed wheat cultivation area predicted with the model ensemble was 2.24 M ha in the 2021 Meher growing season and 2.50 M ha in the 2022 Meher growing season (Figure 3D). The predicted area overestimated the area reported in official statistics by about 13% in 2021 and 8% in 2022. Yet, there were considerable regional differences since the predicted wheat area was comparable to the reported wheat area in Oromia and SNPP regions, but consistently higher in Amhara region. For the Tigray region, the rainfed wheat area was consistent between the ensemble predictions and the official statistics for the 2021, but in 2022 no official statistics were available for model evaluation due to political instability in the region. The rainfed wheat area predicted with the model ensemble was closer to the reported wheat area in official statistics than the area predicted by the individual algorithms (Supplementary Figure S3).

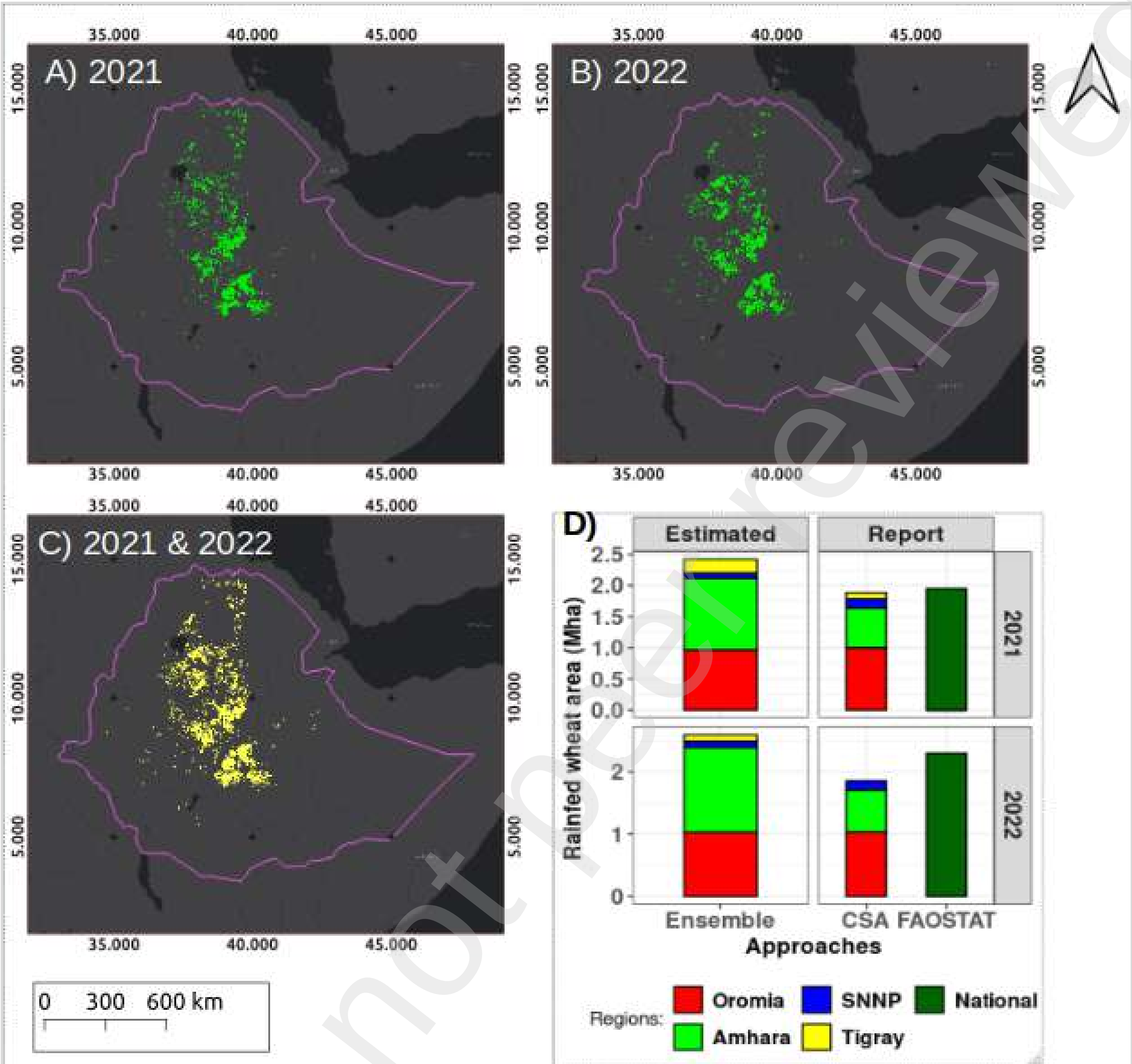

Figure 2 | Rainfed wheat cropland distribution for the 2021 (A) and 2022 (B) Meher growing seasons and for both growing seasons combined (C). Panel (D) displays the predicted wheat area estimated as the sum of the area of each grid cell (10m x 10m) by the total number of grid cells identified as wheat only in relation to official statistics at regional (CSA, 2022) and national levels (FAOSTAT, 2022) for the respective growing seasons. The wheat area distribution maps were produced with an ensemble of gradient boosting (GB), classification and regression tree (CART), and random forest (RF). The ensemble prediction corresponds to the rainfed wheat distribution obtained from the combination of all grid cells consistently classified as wheat by two or three algorithms. Wheat area distribution predicted by each algorithm is provided in Supplementary Figures S3.

3.2. Dynamic ASUs for rainfed wheat in Ethiopia

Three sets of ASUs were produced with both pixel- and object-based cluster approaches for the Ethiopian wheat belt, two were growing season specific for 2021 and 2022 and one was aggregated for the period 2016-2022 (Figure 4). Each set comprised 5 spatial units consistently defined through elbow, silhouette, and BIC metrics (Supplementary Figure S5) to ensure accurate landscape segmentation without oversimplification and excessive fragmentation. This process was informed by the pre-clustering examination of the underlying data structure, which revealed prominent clustering tendencies and distinctive patterns among the features (Supplementary Figure S4).

The two approaches revealed similar spatial patterns in ASUs and exhibited both stability and dynamism in their spatial patterns between the 2021 and 2022 growing seasons (Figures 3 and 4). Considering the pixel-based approach, ASUs 3, 4, and 5 covered about 6%, 28%, and 21% of the rainfed wheat belt, respectively, and had a similar spatial pattern in both growing seasons, indicating stability in production environments over time (Figures 3A, 3C). Conversely, ASU 2 covered a larger share of the rainfed wheat belt in 2022 (27 %) than in 2021 (14%) and the opposite was true for ASU 1 (39 % in 2021 and 24 % in 2022; Figure 3A). Regarding the object-based approach, ASUs 1, 3, and 5 exhibited similar spatial patterns over the two growing seasons (Figures 3B and 3D), but slight differences in area coverage between the seasons, especially ASUs 1 and 5 (Figure 4D). ASU 1 covered 24% of the rainfed belt in 2021 and 15% in 2022, while ASU 5 covered 20% in 2021 and 27% in 2022. ASU 3 covered approximately 15% of the rainfed wheat belt in both growing seasons. Conversely, ASUs 2 and 4 showed changes in spatial pattern over time (Figures 3B and 3D) but maintained nearly the same spatial coverage in both growing seasons, with the latter covering around 19% and the former around 21% of the rainfed wheat belt area (Figure 4D). Results from the aggregate pixel-based ASUs aligned in the geographic extent with ASUs of the two growing seasons for ASUs 2 and 3, but noticeable temporal changes in ASUs 1, 4, and 5. Meanwhile, ASUs delineated with the aggregate object-based approach resulted in temporal stability for ASU 5 and 3 and temporal dynamism for ASUs 1, 2, and 4 compared with the ASUs of the 2022 growing season.

Figures 3G and 3H depict the pixel- and object-based aggregate ASUs confined to the extent of the rainfed wheat area predicted for the 2021 and 2022 growing seasons, respectively. In the pixel-based aggregated ASUs, ASU 4 emerged as the primary environment for rainfed wheat cultivation (Figure 3G), covering about 65% of the rainfed wheat area (Figure 4C), closely followed by ASU 1, which covered 27% of the rainfed wheat area. In the object-based ASUs, ASUs 1 and 5 were the main environments for rainfed wheat cultivation, followed by ASU 4 (Figure 3H). ASUs 1 and 5 covered 43% and 38% of the rainfed wheat area, respectively (Figure 4D). Temporal dynamism between growing seasons was more evident with the pixel-based approach than with the object-based approach (Figures 4C and 4D). The rainfed wheat area covered with ASUs 1, 2, and 3 from the pixel-based approach was about 20% greater in the 2021 growing season than in the 2022 growing season. Such difference in area covered by different ASUs was less evident in the object-based approach. Large differences in area covered were observed between year-specific ASUs and the aggregate ASUs, independently of the clustering approach, indicating that aggregate ASUs were not able to capture year-specific variations in the production environment.

In sum, dynamism in ASUs was less pronounced across the rainfed wheat beltthan t across the rainfed wheat area. This difference was due to shifts in the spatial patterns of ASUs over time, where an ASU might maintain its coverage but change its dominance within or outside the rainfed wheat area. Figures 4A and 4B illustrate these patterns for the wheat belt, while Figures 4C and 4D highlight the changes specific to the rainfed wheat area, emphasizing the varying impacts on ASU coverage and spatial distribution. Temporal dynamism is more pronounced in the pixel-based approach than in the object-based approach for both ASUs and for both thewheat belt level (Figures 3A-3D; Figures 4A and B) and the rain-fed wheat area (Figures 4C and D).

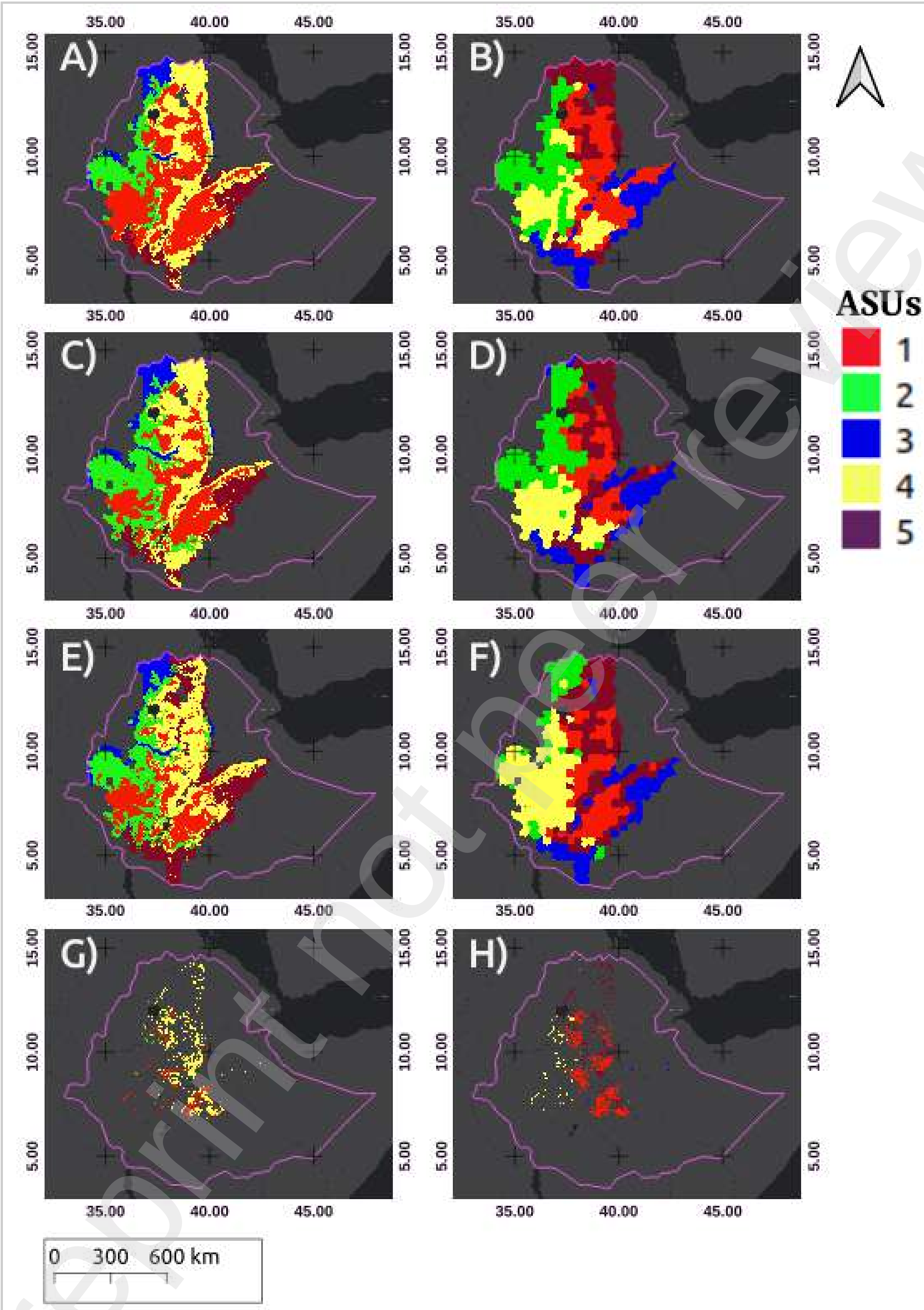

355

Figure 3 | Agroecological spatial units (ASUs) delineated in the Ethiopian rainfed wheat belt using pixel-and object based clustering approaches. Panels (A), (C), and (E) depict pixel-based ASUs for the 2021 and 2022 growing season, and aggregated ASUs derived from time series data for the period 2016-2022, respectively. Panels (B), (D) and (F) exhibit object-based ASUs for the year 2021 and 2022, and aggregated ASUs (2016-2022), respectively. Panels (G) and (H) display aggregate ASUs for the rainfed wheat area only (Figure 2).

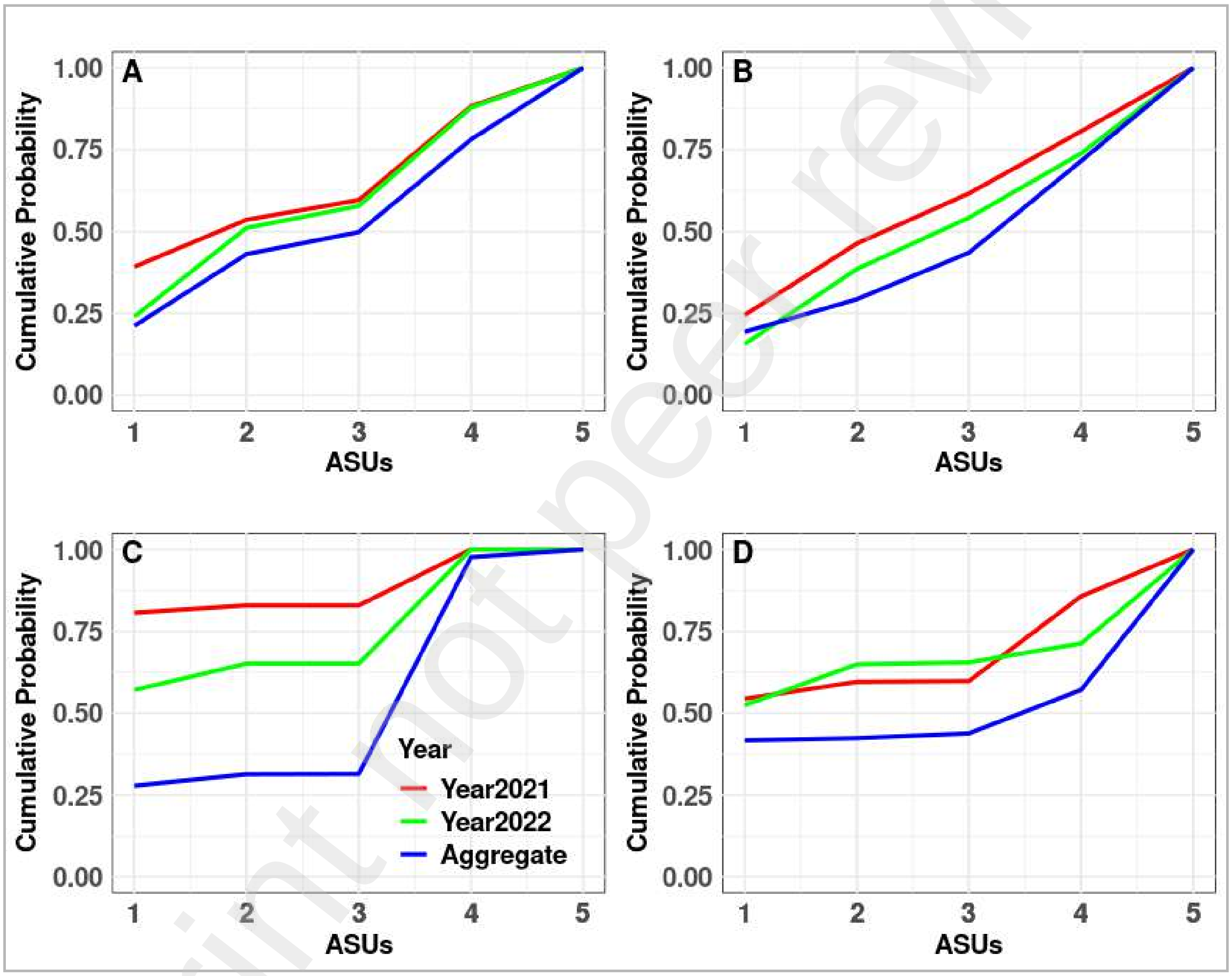

Figure 4 | Cumulative probability plots illustrating the distribution and changes of area covered by ASUs across the rainfed wheat belt (A, B) and the rainfed wheat area (C, D) using pixel- (A, C) and object-based (B, D) clustering approaches.

3.3. Variability between ASUs and clustering performance

The Kruskal-Wallis test revealed highly significant variations in all features across pixel-based ASUs (Figure 5A) and object-based ASUs (Figure 5B), particularly for NDVI, GDD, pH, elevation, and aridity index. The differences were non-significant for temperature seasonality and PAWC (Figure 5B). The separability between ASUs in both approaches was also verified using wheat yield data collected in the 2022 growing season, revealing significant yield differences across ASUs (Supplementary Figure S6). Wheat yield variability between ASUs delineated with object-based clustering (about ~2 t ha $^{-1}$) was found to be significantly different compared to those delineated with pixel-based clustering (about ~0.2 t ha $^{-1}$).

The clustering quality assessment revealed considerable cohesion and separation within and among ASUs, with an average silhouette coefficient of 0.51 for pixel-based ASUs and 0.59 for object-based ASUs (Figures 5C and 5D). For pixel-based ASUs, an average silhouette coefficient of 0.51 indicates that the clusters were moderately well-defined and cohesive and that grid cells within the same cluster were more similar to each other on average than to grid cells in other clusters. The average silhouette coefficient of 0.59 for object-based ASUs reflects a better-defined cluster quality and separation compared to the pixel-based clustering.

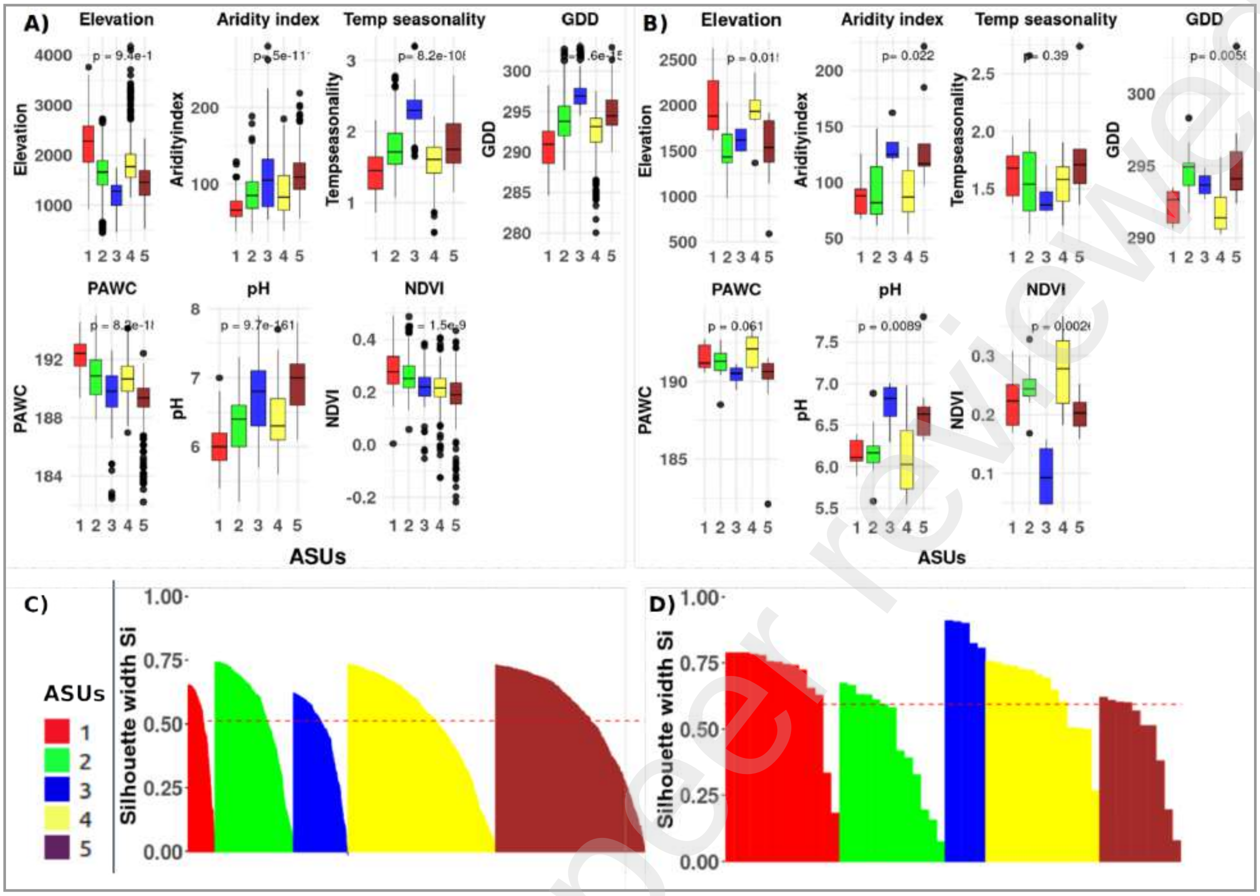

Figure 5 | Internal clustering evaluation illustrating the variability between ASUs and clustering quality for both pixel- and object-based approaches. Panels (A) and (B) display the Kruskal-Wallis test showing the statistical differences between ASUs for pixel- and object-based ASUs, respectively. Panels (C) and (D) display the clustering quality using the silhouette coefficient for both pixel- and object-based approaches, respectively. Each bar in (C) and (D) refers to a grid cell (Figure 4) and dashed lines display the mean silhouette coefficient for each clustering approach.

3.4. Similarity and temporal scalability of dynamic ASUs

The similarity and complementarity between ASUs developed for different time periods with pixel- and object-based approaches is provided in Figure 6. Pixel- and object-based ASUs were mostly similar between each other, but there were also dissimilarities between some of them (Figure 5A). For instance, object-based ASU 1 had a high similarity with pixel-based ASUs 1 and 5, whereas object-based ASU 5 had a high dissimilarity with pixel-based ASU 5. All other pairwise comparisons of ASUs showed more modest levels of (dis)similarity.

The similarity matrix revealed both stability and dynamism between the single-year 2022 and aggregate ASUs in the pixel- and object-based approaches (Figures 6B and 6C). Similarity between ASUs indicates stability whereas dissimilarity between ASUs indicates dynamism across time perspectives. In the pixel-based approach, most aggregate ASUs and single-year ASUs demonstrated a notable degree of stability, except for the observed slight dynamism between ASU 1 across time perspectives (Figure 6B). Conversely, in the object-based approach, only ASUs 1 and 5 showed strong stability between the two-time perspectives, while ASU 4 showed strong dynamism and ASUs 2 and 3 showed a slight dynamism. The analysis suggests that while there is stability between the aggregated and single-year ASUs, there are also specific ASUs (e.g., ASU 1 in the pixel-based approach and ASU 4 in the object-based approach) which are unstable across the time perspectives.

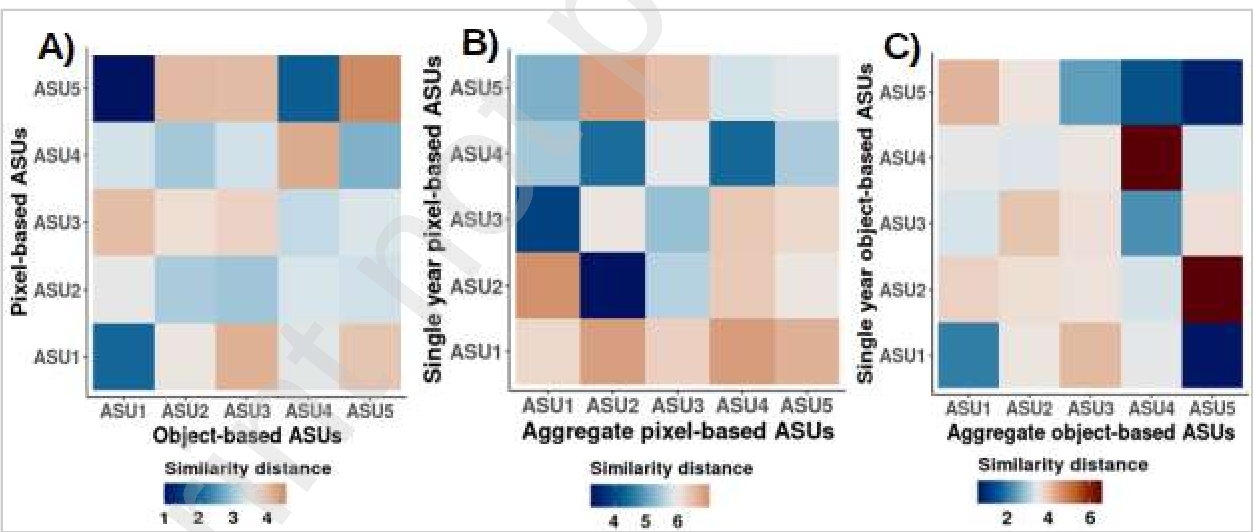

Figure 6 | Similarity and temporal scalability assessment in ASUs produced with different approaches: (A) similarity between aggregate object- and pixel-based ASUs, (B) temporal scalability and dynamism for pixel-based ASUs, and (C) temporal scalability and dynamism for object-based ASUs. Temporal scalability and dynamism considered the

ASUs from the 2022 growing season and the aggregate ASUs. A log-transformation was applied to the original distance matrix to improve readability. A darker shade of blue denotes a stronger similarity between ASUs developed with different approaches, while dark red denotes the opposite.

4. Discussion

4.1. Rainfed wheat area mapping in Ethiopia

We used an ensemble machine learning approach relying on ground truth observations and remote sensing and environmental features to map the annual rainfed wheat distribution at high spatial resolution in Ethiopia. Our approach achieved an overall modeling accuracy of 88% in the 2021 growing season and 94% in the 2022 growing season and the predicted rainfed wheat area was comparable to that reported in official statistics at regional and national levels in two growing seasons (CSA, 2022; FAOSTAT, 2022). The proposed method can therefore be used to generate crop-specific area estimates under smallholder conditions, bringing important advantages over generic crop type distribution data that are not growing season specific (e.g., SPAM2020, You et al., 2024). The higher accuracy observed in this study compared to earlier studies (Eisfelder et al., 2024; Khatami et al., 2020; Delrue et al., 2013;) can be explained by three main methodological aspects.

First, we combined multi-source high-resolution satellite time series images from Sentinel-1 (i.e., radar images) and Sentinel-2 (i.e., optical images), including derived spectral and vegetation indices, as well as seasonal and phenological information, to discriminate rainfed wheat from other crops that have similar spectral signatures (Ofori-Ampofo et al., 2021; Orynbaikyzy et al., 2020). The combination of both images was shown to improve the classification accuracy in other studies as well (Eisfelder et al., 2024; Felegari et al., 2021; Inglada et al., 2016) likely due to better characterization of crop development and environmental cyclical patterns (Ashourloo et al. 2022; Al-Shammari et al. 2020; Ghazaryan et al., 2018;

Lu et al., 2014). Second, environmental data proved important to map the wheat area distribution in addition to remote sensing information as elevation was the most important feature driving the crop area mapping (see also Blickensdörfer et al., 2022; Liu et al., 2020). Finally, the ensemble machine learning approach outperformed the accuracy of the individual algorithms to predict wheat area as also shown in other recent studies (Walhazi et al., 2024; Ahmed et al., 2023; Mahajan et al., 2023; Sagi and Rokach, 2018; Pourdarbani et al., 2019).

Representative and high-quality observational data is critical for model training and to ensure the transferability of our framework to other crops and production environments. Investments in data collection are thus required to build the data stack necessary to generate crop-specific and near real-time crop area distribution maps. Coordinated efforts to assemble geo-referenced ground data (Jolivot et al., 2021) or crowd-sourced data (Wu et al., 2023; See et al., 2013) can help generate the required information for crop type mapping. Assessing the area of applicability of the trained models will also remain important to evaluate where reliable predictions can be made (Meyer and Pebesma, 2021).

4.2. Delineation of ASUs to characterize production environments

The ASUs framework was employed to characterize wheat production environments in Ethiopia considering different clustering algorithms and spatio-temporal aggregation of the input data. Pixel- and object-based ASUs were similar in terms of their characteristics (Figure 6A) and spatial arrangement (Figure 4 A-F) and so was the consistency between single-year and aggregate ASUs (Figures 6B and 6C). Internal and external evaluation metrics demonstrated the reliability of the framework to segment production environments. For instance, ASUs 1 identified with pixel-based clustering captured topographic and environmental conditions associated with the highland regions of the Ethiopian wheat belt. These include elevated terrain, high vegetation index, ample plant-available water holding capacity, and low degree of temperature seasonality and low growing degree days.

Our approach to develop ASUs balanced the trade-off between oversimplification and excessive fragmentation of production environments through the exploration of similarities between grid cells (Figure S3) and the data-driven definition of the optimum number of ASUs. As such, the ASUs were delineated such that climatic homogeneity within zones was achieved while minimizing the number of zones required to capture significant portions of the cultivated area of the target crop. The ASUs framework thus offered advantages over previous studies relying on matrix zonation derived from expert knowledge (e.g., Edreira et al., 2018; van Wart et al., 2013; Mueller et al., 2012;). Lobell (2013) highlighted the need to keep the spatial units small enough to minimize within unit climate variations but large enough to reduce the costs of data collection for yield gap analysis.

Combining pixel and object-based approaches ensured spatial scalability that can be adaptable for characterization of production environments across spatial scales. Pixel-based ASUs unveiled spatial patterns at high resolution (Figure 4A-C), which could be suitable for agronomic assessments at local level (e.g., Stuart et al., 2016). Conversely, object-based ASUs resulted in coarser yet more interpretable ASUs (Figure 4D-F), hence offering opportunities for agronomic assessments at national to global level. This flexibility to generate high-resolution and coarser ASUs is an important feature of our data-driven approach, which can be attuned to the spatial scale most suitable to the analysis at hand. As shown in Figure 6A, pixel-based ASUs 3, 4 and 5 differed from their object-based counterparts, indicating these two approaches are not mutually exclusive. This distinction underscores the complementary of the two methods such that using both approaches leads to a more comprehensive understanding of the production environment.

The delineated ASUs with both pixel- and object-based approaches were temporally scalable yet dynamic. There was a consistent agreement between aggregate ASUs and year-specific ASUs, which indicates similarities in longer-term and short-term variations in the production environments for rainfed wheat in

Ethiopia. Such agreement between different time perspectives is likely different in e.g., semi-arid environments with high rainfall variability, which remains to be tested in future. Yet, some of the ASUs (e.g., ASU 1 from pixel-based and ASU 4 from object-based approach) changed across time perspectives, indicating the ability of the framework to capture changes in crop production environments. Our findings thus address earlier concerns regarding the relevance of a temporally scalable framework for agronomic analysis (e.g., Sadras et al., 2015; Lobell et al., 2013).

4.3. Relevance and transferability of the ASUs framework

Wheat is a strategic crop for food security in Ethiopia, where farmers' yields remain well below what is biophysically possible with improved agronomic practices and import dependency poses a heavy burden on the national economy (Silva et al., 2023; Senbeta et al., 2023; Tadesse et al., 2022; Silva et al., 2021). Narrowing wheat yield gaps is therefore high on the agenda of national policies. The ASUs developed in this paper provide a first step to characterize Ethiopia's wheat production environments in the context of yield gap analysis for wheat in the country. The approach followed for ASU delineation offered spatial units grounded in relevant agro-ecological attributes, which could facilitate agronomic assessments of wheat productivity and resource- use efficiency across different spatial and temporal scales. For instance, pixel- based ASUs could support context-specific yield gap analyses (e.g., Stuart et al., 2016) or targeting fertilizer advisories across the rainfed wheat belt (Liben et al., 2024) for which short-term and localized environmental characterization is required. Conversely, object-based ASUs could support large-scale yield gap analyses aiming to inform food security and climate change assessments at supra-national level (Alimagham et al., 2024; van Ittersum et al., 2016). More broadly, the ASUs framework can also inform the tailoring of agricultural technologies to local contexts when combined with socio-economic data (Muthoni et al., 2017; Tesfaye et al., 2015), and the ex-ante evaluation of agricultural technologies across spatial scales (Andrade et al., 2019), among others.

The ASUs framework developed and tested in this study can be adaptable and transferable to other crops and regions with minor modifications. For instance, feature engineering will require crop-specific adjustments that are also context-specific when aiming to transfer the ASUs framework to other regions. This will be especially important for remote sensing-derived features (seasonal parameters and vegetation indices) and environmental data which are crop- and growing season-specific (Supplementary Table 1). Including time series information for time-variant features will remain important to ensure temporal transferability and capture inter- and intra-annual variations in the production environment. From a methodological standpoint, conducting pre-cluster data exploration and defining the optimum number of clusters in a data-driven way is required to avoid both oversimplification and hyper-segmentation of production environments, which could also be achieved using dynamic clustering algorithms (Zhang and Hepner, 2017). As clustering analysis is computationally intensive, cloud computing platforms like Google Earth Engine will be necessary. Finally, we recommend assembling data stacks with ground truth observations on crop type presence and measured crop yields to be able to generate accurate crop type maps and evaluate the performance of the clustering analysis in data-rich regions. Internal evaluation techniques based on dissimilarity analysis across the feature space would be recommended for data-poor regions (Hardy et al., 2011; Brun et al., 2007).

5. Conclusion

We developed data-driven crop-specific, and time-variant agro-ecological spatial units (ASUs) that can facilitate the characterization of crop production environments. The framework entailed the mapping of rainfed wheat areas in Ethiopia during the 2021 and 2022 growing seasons based on ensemble machine learning and multi-source time series satellite images, derived vegetation indices, and environmental data, and the delineation of crop-specific time variant ASUs using pixel- and object-based clustering algorithms. The model ensemble predicted the distribution of rainfed wheat areas in Ethiopia accurately, achieving high classification accuracy (>90%) and strong generalizability over the two growing seasons. The rainfed wheat area estimates for 2021 and 2022 were 2.24 and 2.50 million hectares, respectively, a 10% deviation above reports in official statistics. ASUs were developed using pixel- and object-based clustering approaches in Ethiopia's rainfed wheat belt. While the spatial scalability of ASUs could support the characterization of production environments across spatial scales, its temporal dynamism could support the analysis of longer-term trends and short-term fluctuations in the production environment. This spatio-temporal flexibility allows the framework to capture the change in crop production environment over both space and time to inform responses to essential food security and environmental challenges. The framework developed in this study can be adaptable and transferable to other crops and regions in a cost-effective way where ground truth observations are readily available. This adaptability allows for a broader relevance including scaling out agronomic findings and technologies to a broader geographic scale, hence supporting sustainable crop intensification in complex production environments.

Declaration of competing interest

We declare that there is no conflict of interest associated with all co-authors.

CRediT authorship statement

HSG: Conceptualization, Methodology, Data curation, Software, Investigation, Formal analysis; Writing-original draft, Review & Editing. **LL:** Conceptualization, Methodology, Writing-original draft, Review & Editing, Investigation, Supervision, Project administration, Funding acquisition. **LT:** Conceptualization, Writing - Review & Editing, Supervision. **MTC:** Conceptualization, Writing - Review & Editing. **GB:** Data curation, Writing - Review & Editing. **DT:** Data curation, Writing - Review & Editing. **WA:** Conceptualization, Review & Editing. **TS:** Data curation, Review & Editing **KT**: Data curation,Review & Editing. **MC:** Conceptualization, Writing - Review & Editing, Supervision, Project administration, Funding acquisition.**JVS:** Conceptualization, Writing-original draft, Review & Editing, Visualization.

Acknowledgments

This study was funded by the OneCGIAR Research Excellence in Agronomy Initiative (INV-005431). Habtamu Gelagay received a fellowship from the French Space Agency (CNES) and was supported by the French National Research Agency under the Investments for the Future Program (ANR-16-CONV-0004). The authors wish to thank CIAT-Ethiopia and CIMMYT-Ethiopia for providing the ground-truth observations used in this study.

Data availability

All the geospatial data used are freely available under Google Earth Engine (https://developers.google.com/earth-engine/datasets/catalog). Data produced by this study namely wheat crop area and the ASUs will be made available upon request.

Reference

Abatzoglou, J. T., Dobrowski, S. Z., Parks, S. A., & Hegewisch, K. C. (2018). TerraClimate, a high-resolution global dataset of monthly climate and climatic water balance from 1958–2015. *Scientific data*, *5*(1), 1-12.

Ahmed, S., Mahmoud, A. S., Farg, E., Mohamed, A. M., Moustafa, M. S., Abutaleb, K., Saleh, A. M.,AbdelRahman, M. A. E., AbdelSalam, H. M., & Arafat, S. M. (2023). Investigation on the use of ensemble learning and big data in crop identification. *Heliyon*, *9*(2), e13339. https://doi.org/10.1016/j.heliyon.2023.e13339

Alimagham, S., van Loon, M. P., Ramirez-Villegas, J., Adjei-Nsiah, S., Baijukya, F., Bala, A., ... & van Ittersum, M. K. (2024). Climate change impact and adaptation of rainfed cereal crops in sub-Saharan Africa. *European Journal of Agronomy*, *155*, 127137.

Al-Shammari, D., Fuentes, I., M. Whelan, B., Filippi, P., & FA Bishop, T. (2020). Mapping of cotton fields within-season using phenology-based metrics derived from a time series of landsat imagery. *Remote Sensing,* 12(18), 3038.

Amede, T., Gashaw, T., Legesse, G., Tamene, L., Mekonen, K., Thorne, P., & Schultz, S. (2022). Landscape positions dictating crop fertilizer responses in wheat-based farming systems of East African Highlands. *Renewable Agriculture and Food Systems*, *37*(S1), S4–S16. https://doi.org/10.1017/S1742170519000504

Andrade, J. F., Edreira, J. I. R., Farrow, A., van Loon, M. P., Craufurd, P. Q., Rurinda, J., ... & Grassini, P. (2019). A spatial framework for ex-ante impact assessment of agricultural technologies. *Global Food Security*, *20*, 72-81.

Ashourloo, D., Nematollahi, H., Huete, A., Aghighi, H., Azadbakht, M., Shahrabi, H. S., Goodarzdashti, S. (2022). A new phenology-based method for mapping wheat and barley using time-series of Sentinel-2 images. *Remote Sensing of Environment*, *280*, 113206. https://doi.org/10.1016/j.rse.2022.113206

Aslam, M. A., Ahmed, M., Stöckle, C. O., Higgins, S. S., Hassan, F. U., & Hayat, R. (2017). Can growing degree days and photoperiod predict spring wheat phenology?. *Frontiers in Environmental Science,* 5, 57.

Arthur, D., & Vassilvitskii, S. (2007). k-means++: The advantages of careful seeding. In Soda (Vol. 7, pp. 1027-1035).

Araya, A., Keesstra, S. D., & Stroosnijder, L. (2010). A new agro-climatic classification for crop suitability zoning in northern semi-arid Ethiopia. *Agricultural and forest meteorology*, *150*(7-8), 1057-1064.

Ayyoob, M. P. (2015). Tools Pros and Cons of Clustering Algorithms using Weka Tools. In International Journal of Computer Applications: National Conference on Advances in Computing Communication and Application, pp-13 (Vol. 16).

Bahmani, B., Moseley, B., Vattani, A., Kumar, R., & Vassilvitskii, S. (2012). Scalable k-means++. arXiv preprint arXiv:1203.6402.

Beckham, C., Hall, M., & Frank, E. (2016). WekaPyScript: Classification, regression, and filter schemes for WEKA implemented in Python. *Journal of Open Research Software*, *4*(1), e33-e33.

Beza, E., Silva, J. V., Kooistra, L., & Reidsma, P. (2017). Review of yield gap explaining factors and opportunities for alternative data collection approaches. *European Journal of Agronomy*, *82*, 206–222. https://doi.org/10.1016/j.eja.2016.06.016

Blickensdörfer, L., Schwieder, M., Pflugmacher, D., Nendel, C., Erasmi, S., & Hostert, P. (2022). Mapping of crop types and crop sequences with combined time series of Sentinel-1, Sentinel-2 and Landsat 8 data for Germany. *Remote Sensing of Environment*, *269*, 112831. https://doi.org/10.1016/j.rse.2021.112831

Breiman, L. (2001). Random Forests. *Machine Learning*, *45*(1), 5–32. https://doi.org/10.1023/A:1010933404324

Breimann, L., Friedman, J. H., Olshen, R. A., & Stone, C. J. (1984). Classification and regression trees. *Pacific Grove, Wadsworth*.

Brock, G., Pihur, V., Datta, S., & Datta, S. (2008). clValid: An R package for cluster validation. *Journal of statistical*

Software, *25*, 1-22.
Brun, M., Sima, C., Hua, J., Lowey, J., Carroll, B., Suh, E., & Dougherty, E. R. (2007). Model-based evaluation of clustering validation measures. *Pattern Recognition*, *40*(3), 807–824. https://doi.org/10.1016/j.patcog.2006.06.026
Bui, Q. T., Chou, T. Y., Hoang, T. V., Fang, Y. M., Mu, C. Y., Huang, P. H., ... & Meadows, M. E. (2021). Gradient boosting machine and object-based CNN for land cover classification. Remote Sensing,
Cao, F., Liang, J., Li, D., Bai, L., & Dang, C. (2012). A dissimilarity measure for the k-Modes clustering algorithm. *Knowledge-Based Systems*, *26*, 120–127. https://doi.org/10.1016/j.knosys.2011.07.011
Cassman, K. G. (1999). Ecological intensification of cereal production systems: Yield potential, soil quality, and precision agriculture. *Proceedings of the National Academy of Sciences*, *96*(11), 5952–5959. https://doi.org/10.1073/pnas.96.11.5952
Cassman, K. G., & Grassini, P. (2020). A global perspective on sustainable intensification research. *Nature sustainability*, *3*(4), 262-268.
Central Statistical Agency (2021). The Federal Democratic Republic of Ethiopia Central Statistical Agency, Agricultural Sample Survey (2013 E.C.), volume I, report on area and production of major crops (private peasant holdings, meher season) statistical bulletin 590. Addis Ababa, Ethiopia.
Central Statistical Agency (2021). The Federal Democratic Republic of Ethiopia Central Statistical Agency, Agricultural Sample Survey (2014 E.C.), volume I, report on area and production of major crops (private peasant holdings, meher season) statistical bulletin 593. Addis Ababa, Ethiopia.
Defourny, P., Bontemps, S., Bellemans, N., Cara, C., Dedieu, G., Guzzonato, E., Hagolle, O., Inglada, J., Nicola, L., Rabaute, T., Savinaud, M., Udroiu, C., Valero, S., Bégué, A., Dejoux, J.-F., El Harti, A., Ezzahar, J., Kussul, N., Labbassi, K., … Koetz, B. (2019). Near real-time agriculture monitoring at national scale at parcel resolution: Performance assessment of the Sen2-Agri automated system in various cropping systems around the world. *Remote Sensing of Environment*, *221*, 551–568. https://doi.org/10.1016/j.rse.2018.11.007
Delrue, J., Bydekerke, L., Eerens, H., Gilliams, S., Piccard, I., & Swinnen, E. (2013). Crop mapping in countries with small-scale farming: A case study for West Shewa, Ethiopia. *International Journal of Remote Sensing*. https://www.tandfonline.com/doi/abs/10.1080/01431161.2012.747016
Digital Earth Africa (DEA),(2021). Cropland extent maps for Africa. https://docs.digitalearthafrica.org/en/latest/data_specs/Cropland_extent_specs.html)
Di Falco, S., Chavas, J. P., & Smale, M. (2007). Farmer management of production risk on degraded lands: the role of wheat variety diversity in the Tigray region, Ethiopia. *Agricultural Economics,* 36(2), 147-156.
Dutta, A., Dutta, S. K., Jena, S., Nath, R., Bandyopadhyay, P., & Chakraborty, K. (2011). Effect of growing degree days on biological growth indices of wheat and mustard. *Journal of Crop and Weed*, 7(1), 70-76.
Edreira, J. I. R., Cassman, K. G., Hochman, Z., Van Ittersum, M. K., Van Bussel, L., Claessens, L., & Grassini, P. (2018). Beyond the plot: technology extrapolation domains for scaling out agronomic science. *Environmental Research Letters*, *13*(5), 054027
Effa, K., Fana, D. M., Nigussie, M., Geleti, D., Abebe, N., Dechassa, N., ... & Berisso, F. E. (2023). The irrigated wheat initiative of Ethiopia: a new paradigm emulating Asia's green revolution in Africa. *Environment, Development and Sustainability*, 1-26..
Eisfelder, C., Boemke, B., Gessner, U., Sogno, P., Alemu, G., Hailu, R., Mesmer, C., & Huth, J. (2024). Cropland and Crop Type Classification with Sentinel-1 and Sentinel-2 Time Series Using Google Earth Engine for Agricultural Monitoring in Ethiopia. *Remote Sensing*, *16*(5), 5. https://doi.org/10.3390/rs16050866
Eck, M. A., Murray, A. R., Ward, A. R., & Konrad, C. E. (2020). Influence of growing season temperature and precipitation anomalies on crop yield in the southeastern United States. *Agricultural and Forest Meteorology*, 291, 108053.
Farr, T. G., Rosen, P. A., Caro, E., Crippen, R., Duren, R., Hensley, S., ... & Alsdorf, D. (2007). The shuttle radar topography mission. *Reviews of geophysics*, *45*(2).
Felegari, S., Sharifi, A., Moravej, K., Amin, M., Golchin, A., Muzirafuti, A., Tariq, A., & Zhao, N. (2021). Integration of Sentinel 1 and Sentinel 2 Satellite Images for Crop Mapping. *Applied Sciences*, *11*(21), 21. https://doi.org/10.3390/app112110104
Field, Z., Miles, J., & Field, A. (2012). Discovering Statistics Using R, 1-992.
Food and Agricultural Organization (FAO), 1978. Report on the agro-ecological zones project. FAO, Rome.
Food and Agriculture Organization of the United Nations. (2022). FAOSTAT: Crop and livestock database. Retrieved

January 25, 2024, from https://www.fao.org/faostat/en/#data/QCL.

Fraley, C., & Raftery, A. E. (1998). How many clusters? Which clustering method? Answers via model-based cluster analysis. T*he computer journal, 41(8), 578-588*

Friedman, J.H., (2001). Greedy function approximation: a gradient boosting machine. Annals of statistics, pp.1189-1232.

Fritz, S., See, L., McCallum, I., You, L., Bun, A., Moltchanova, E., Duerauer, M., Albrecht, F., Schill, C., Perger, C., Havlik, P., Mosnier, A., Thornton, P., Wood-Sichra, U., Herrero, M., Becker-Reshef, I., Justice, C., Hansen, M., Gong, P., … Obersteiner, M. (2015). Mapping global cropland and field size. *Global Change Biology*, *21*(5), 1980–1992. https://doi.org/10.1111/gcb.12838

Funk, C., Peterson, P., Landsfeld, M., Pedreros, D., Verdin, J., Shukla, S., ... & Michaelsen, J. (2015). The climate hazards infrared precipitation with stations—a new environmental record for monitoring extremes. *Scientific data*, *2*(1), 1-21.

Gangadhara Bhat, H., & Moges, D. M. (2021). Climate change and its implications for rainfed agriculture in Ethiopia.*J. Water Clim. Change*,*12*, 1229-1244.

Gao, X. (2010). Composite Likelihood Bayesian Information Criteria for Model Selection in High-Dimensional Data. *Journal of the American Statistical Association*.

Ghazaryan, G., Dubovyk, O., Löw, F., Lavreniuk, M., Kolotii, A., Schellberg, J., & Kussul, N. (2018). A rule-based approach for crop identification using multi-temporal and multi-sensor phenological metrics. *European Journal of Remote Sensing*, *51*(1), 511–524. https://doi.org/10.1080/22797254.2018.1455540

Gorelick, N., Hancher, M., Dixon, M., Ilyushchenko, S., Thau, D., & Moore, R. (2017). Google Earth Engine: Planetary-scale geospatial analysis for everyone. *Remote Sensing of Environment*, *202*, 18–27. https://doi.org/10.1016/j.rse.2017.06.031

Grassini, P., Pittelkow, C. M., Cassman, K. G., Yang, H. S., Archontoulis, S., Licht, M., ... & Guindin-Garcia, N. (2017). Robust spatial frameworks for leveraging research on sustainable crop intensification. *Global food security*, *14*, 18-22.

Grassini, P., van Bussel, L. G. J., Van Wart, J., Wolf, J., Claessens, L., Yang, H., Boogaard, H., de Groot, H., van Ittersum, M. K., & Cassman, K. G. (2015). How good is good enough? Data requirements for reliable crop yield simulations and yield-gap analysis. *Field Crops Research*, *177*, 49–63. https://doi.org/10.1016/j.fcr.2015.03.004

Green, P. E., & Rao, V. R. (1969). A note on proximity measures and cluster analysis.

Grossman, R. B., & Reinsch, T. G. (2002). 2.1 Bulk density and linear extensibility. *Methods of soil analysis: Part 4 physical methods*, *5*, 201-228.

Hardy Kremer, Philipp Kranen, Timm Jansen, Thomas Seidl, Albert Bifet, Geoff Holmes, and Bernhard Pfahringer. (2011). An effective evaluation measure for clustering on evolving data streams. In ACM SIGKDD, pages 868–876.

Headey, D., Dereje, M., & Taffesse, A. S. (2014). Land constraints and agricultural intensification in Ethiopia: A village-level analysis of high-potential areas. *Food Policy*, *48*, 129–141. https://doi.org/10.1016/j.foodpol.2014.01.008

Hengl, T., Miller, M. A., Križan, J., Shepherd, K. D., Sila, A., Kilibarda, M., ... & Crouch, J. (2021). African soil properties and nutrients mapped at 30 m spatial resolution using two-scale ensemble machine learning. *Scientific reports*, *11*(1), 6130.

Hordofa, A. T., Leta, O. T., Alamirew, T., & Chukalla, A. D. (2022). Response of Winter Wheat Production to Climate Change in Ziway Lake Basin. *Sustainability*, *14*(20), 20. https://doi.org/10.3390/su142013666

Inglada, J., Vincent, A., Arias, M., & Marais-Sicre, C. (2016). Improved Early Crop Type Identification By Joint Use of High Temporal Resolution SAR And Optical Image Time Series. *Remote Sensing*, *8*(5), 5. https://doi.org/10.3390/rs8050362

Jakubauskas, M. E., Legates, D. R., & Kastens, J. H. (2001). Harmonic analysis of time-series AVHRR NDVI data. *Photogrammetric engineering and remote sensing*, *67*(4), 461-470.

Jakubauskas, M. E., Legates, D. R., & Kastens, J. H. (2002). Crop identification using harmonic analysis of time-series AVHRR NDVI data. *Computers and Electronics in Agriculture*, *37*(1), 127–139. https://doi.org/10.1016/S0168-1699(02)00116-3

Jones, Richard H. "Bayesian information criterion for longitudinal and clustered data." *Statistics in medicine* 30, no. 25 (2011): 3050-3056.

Jolivot, A., Lebourgeois, V., Ameline, M., Andriamanga, V., Bellón, B., Castets, M., ... & Bégué, A. (2021). Harmonized in situ JECAM datasets for agricultural land use mapping and monitoring in tropical countries. *Earth System Science Data Discussions*, *2021*, 1-22.

Jonsson, P., & Eklundh, L. (2002). Seasonality extraction by function fitting to time-series of satellite sensor data. *IEEE Transactions on Geoscience and Remote Sensing*, *40*(8), 1824–1832. https://doi.org/10.1109/TGRS.2002.802519

Kassawmar, T., Eckert, S., Hurni, K., Zeleke, G., & Hurni, H. (2018). Reducing landscape heterogeneity for improved land use and land cover (LULC) classification across the large and complex Ethiopian highlands. *Geocarto international*, *33*(1), 53-69.

Kaufman, L. and Rousseeuw, P.J. (2009). Finding Groups in Data: An Introduction to Cluster Analysis (Vol. 344). New York: John Wiley & Sons. ISBN: 0-471-87876-6 Google Scholar.

Klein, T., Holzkämper, A., Calanca, P., Seppelt, R., & Fuhrer, J. (2013). Adapting agricultural land management to climate change: a regional multi-objective optimization approach. *Landscape ecology*, *28*, 2029-2047.

Khatami, R., Southworth, J., Muir, C., Caughlin, T., Ayana, A. N., Brown, D. G., ... & Agrawal, A. (2020). Operational large-area land-cover mapping: an Ethiopia case study. *Remote Sensing*, *12*(6), 954.

Kouadio, L., and Newlands, N. K. (2015). Building capacity for assessing spatial-based sustainability metrics in agriculture. *Decision Analytics*, *2*, 1-18.

Kruskal, W. H., & Wallis, W. A. (1952). Use of ranks in one-criterion variance analysis. *Journal of the American Statistical Association,* 47(260), 583-621.

Kumhálová, J., Matejkova, S., Fifernová, M., Lipavsky, J., & Kumhála, F. (2008). Topography impacts on nutrition content in soil and yield. *Plant Soil and Environment*, *54*(6), 255.

Kwedlo, W. (2011). A clustering method combining differential evolution with the *K*-means algorithm. *Pattern Recognition Letters*, *32*(12), 1613–1621. https://doi.org/10.1016/j.patrec.2011.05.010

Landis, J. R., & Koch, G. G. (1977). The Measurement of Observer Agreement for Categorical Data. *Biometrics*, *33*(1), 159–174. https://doi.org/10.2307/2529310

Li, C., Cai, R., Tian, W., Yuan, J., & Mi, X. (2023). Land cover classification by Gaofen satellite images based on CART algorithm in Yuli County, Xinjiang, China. *Sustainability*, *15*(3), 2535.

Liben, F., Abera, W., Chernet, M. T., Ebrahim, M., Tilaye, A., Erkossa, T., ... & Tamene, L. (2024). Site-specific fertilizer recommendation using data driven machine learning enhanced wheat productivity and resource use efficiency. *Field Crops Research*, *313*, 109413.

Liu, X., Zhai, H., Shen, Y., Lou, B., Jiang, C., Li, T., Hussain, S. B., & Shen, G. (2020). Large-Scale Crop Mapping From Multisource Remote Sensing Images in Google Earth Engine. *IEEE Journal of Selected Topics in Applied Earth Observations and Remote Sensing*, *13*, 414–427. https://doi.org/10.1109/JSTARS.2019.296353

Lobell, D. B. (2013). The use of satellite data for crop yield gap analysis. *Field Crops Research*, *143*, 56–64. https://doi.org/10.1016/j.fcr.2012.08.008

Lu, L., Wang, C., Guo, H., & Li, Q. (2014). Detecting winter wheat phenology with SPOT-VEGETATION data in the North China Plain. *Geocarto International*. https://www.tandfonline.com/doi/abs/10.1080/10106049.2012.760004

Mahajan, P., Uddin, S., Hajati, F., & Moni, M. A. (2023). Ensemble Learning for Disease Prediction: A Review. *Healthcare*, *11*(12), 12. https://doi.org/10.3390/healthcare11121808

Mercier, A., Betbeder, J., Rapinel, S., Jegou, N., Baudry, J., & Hubert-Moy, L. (2020). Evaluation of Sentinel-1 and -2 time series for estimating LAI and biomass of wheat and rapeseed crop types. *Journal of Applied Remote Sensing*, *14*(2), 024512. https://doi.org/10.1117/1.JRS.14.024512

Metzger, M. J., Bunce, R. G., Jongman, R. H., Sayre, R., Trabucco, A., & Zomer, R. (2013). A high-resolution bioclimate map of the world: A unifying framework for global biodiversity research and monitoring. *Global Ecology and Biogeography,* 22(5), 630-638.

Meyer, H., & Pebesma, E. (2021). Predicting into unknown space? Estimating the area of applicability of spatial prediction models. *Methods in Ecology and Evolution*, *12*(9), 1620-1633.

Mi, L., & Chen, Z. (2020). Superpixel-enhanced deep neural forest for remote sensing image semantic segmentation. *ISPRS Journal of Photogrammetry and Remote Sensing*, *159*, 140-152.

Mohammed, I. M. A. (2019). *Mapping crop field probabilities using hyper temporal and multi spatial remote sensing in a fragmented landscape of Ethiopia* (Master's thesis, University of Twente).

Mueller, N. D., Gerber, J. S., Johnston, M., Ray, D. K., Ramankutty, N., & Foley, J. A. (2012). Closing yield gaps through nutrient and water management. *Nature*, *490*(7419), 254–257. https://doi.org/10.1038/nature11420

Muñoz Sabater, J., (2019): ERA5-Land monthly averaged data from 1981 to present. Copernicus Climate Change Service (C3S) Climate Data Store (CDS). doi:10.24381/cds.68d2bb30

Muthoni, F. K., Guo, Z., Bekunda, M., Sseguya, H., Kizito, F., Baijukya, F., & Hoeschle-Zeledon, I. (2017). Sustainable recommendation domains for scaling agricultural technologies in Tanzania. *Land Use Policy*, *66*, 34–48. https://doi.org/10.1016/j.landusepol.2017.04.028

Neath, A. A., and Cavanaugh, J. E. (2012). The Bayesian information criterion: background, derivation, and applications. *Wiley Interdisciplinary Reviews: Computational Statistics*, *4*(2), 199-203.

Negisho, K., Shibru, S., Matros, A., Pillen, K., Ordon, F., & Wehner, G. (2022). Association Mapping of Drought Tolerance Indices in Ethiopian Durum Wheat (Triticum turgidum ssp. Durum). *Frontiers in Plant Science*, *13*. https://doi.org/10.3389/fpls.2022.838088

Ofori-Ampofo, S., Pelletier, C., & Lang, S. (2021). Crop Type Mapping from Optical and Radar Time Series Using Attention-Based Deep Learning. *Remote Sensing*, *13*(22), 4668. https://doi.org/10.3390/rs13224668

Orynbaikyzy, A., Gessner, U., & Conrad, C. (2019). Crop type classification using a combination of optical and radar remote sensing data: A review. *International Journal of Remote Sensing*, *40*(17), 6553–6595. https://doi.org/10.1080/01431161.2019.1569791

Orynbaikyzy, A., Gessner, U., Mack, B., & Conrad, C. (2020). Crop Type Classification Using Fusion of Sentinel-1 and Sentinel-2 Data: Assessing the Impact of Feature Selection, Optical Data Availability, and Parcel Sizes on the Accuracies. *Remote Sensing*, *12*(17), 17. https://doi.org/10.3390/rs12172779

Pelleg, D., & Moore, A. W. (2000, June). X-means: Extending k-means with efficient estimation of the number of clusters. In Icml (Vol. 1, pp. 727-734).

Pishro-Nik, H. (2014). *Introduction to probability, statistics, and random processes* (p. 732). Blue Bell, PA, USA: Kappa Research, LLC.

Porter, J. R., & Semenov, M. A. (2005). Crop responses to climatic variation. *Philosophical Transactions of the Royal Society B: Biological Sciences*, *360*(1463), 2021–2035. https://doi.org/10.1098/rstb.2005.1752

Pourdarbani, R., Sabzi, S., Hernández-Hernández, M., Hernández-Hernández, J. L., García-Mateos, G., Kalantari, D., & Molina-Martínez, J. M. (2019). Comparison of Different Classifiers and the Majority Voting Rule for the Detection of Plum Fruits in Garden Conditions. *Remote Sensing*, *11*(21), 21. https://doi.org/10.3390/rs11212546

Puzicha, J., Hofmann, T., & Buhmann, J. M. (2000). A theory of proximity based clustering: Structure detection by optimization. *Pattern Recognition*, *33*(4), 617–634. https://doi.org/10.1016/S0031-3203(99)00076-X

Ramirez-Villegas, J., & Challinor, A. (2012). Assessing relevant climate data for agricultural applications. *Agricultural and Forest Meteorology*, *161*, 26–45.https://doi.org/10.1016/j.agrformet.2012.03.015

Rockström, J., Williams, J., Daily, G., Noble, A., Matthews, N., Gordon, L., ... & Smith, J. (2017). Sustainable intensification of agriculture for human prosperity and global sustainability. *Ambio*, *46*, 4-17.

Rouse, J. W., Haas, R. H., Schell, J. A., & Deering, D. W. (1974). Monitoring vegetation systems in the Great Plains with ERTS. NASA Spec. Publ, 351(1), 309.

Rousseeuw, P. J. (1987). Silhouettes: A graphical aid to the interpretation and validation of cluster analysis. *Journal of Computational and Applied Mathematics*, *20*, 53–65. https://doi.org/10.1016/0377-0427(87)90125-7

Sagi, O., & Rokach, L. (2018). Ensemble learning: A survey. *Wiley interdisciplinary reviews: data mining and knowledge discovery*, *8*(4), e1249.

Sadras, V., Cassman, K., Grassini, P., Bastiaanssen, W., Laborte, A., Milne, A., Sileshi, G., & Steduto, P. (2015). Yield gap analysis of field crops: Methods and case studies. *Daugherty Water for Food Global Institute: Faculty Publications*. https://digitalcommons.unl.edu/wffdocs/87

See, L., Fritz, S., You, L., Ramankutty, N., Herrero, M., Justice, C., Becker-Reshef, I., Thornton, P., Erb, K., Gong, P., Tang, H., van der Velde, M., Ericksen, P., McCallum, I., Kraxner, F., Obersteiner, M., (2015). Improved global cropland data as an essential ingredient for food security. *Global Food Security.* 4, 37–45

See, L., McCallum, I., Fritz, S., Perger, C., Kraxner, F., Obersteiner, M., ... & Ram Kalita, N. (2013). Mapping cropland in Ethiopia using crowdsourcing. *International Journal of Geosciences*, *4*(6), 6-13

Senbeta, A. F., & Worku, W. (2023). Ethiopia's wheat production pathways to self-sufficiency through land area expansion, irrigation advance, and yield gap closure. Heliyon, 9(10). https://doi.org/10.1016/j.heliyon.2023.e20720

Silva, J. V., Jaleta, M., Tesfaye, K., Abeyo, B., Devkota, M., Frija, A., ... & Baudron, F. (2023). Pathways to wheat self-sufficiency in Africa. *Global Food Security*, *37*, 100684.

Silva, J. V., Reidsma, P., Baudron, F., Jaleta, M., Tesfaye, K., & van Ittersum, M. K. (2021). Wheat yield gaps across smallholder farming systems in Ethiopia. *Agronomy for Sustainable Development*, *41*(1), 12.

Simane, B., Tanner, D. G., Tarekegne, A. T., & Taa, A. (1999). Agro-ecological decision support systems for wheat improvement in Ethiopia: climatic characterisation and clustering of wheat growing regions.

Stuart, A. M., Pame, A. R. P., Silva, J. V., Dikitanan, R. C., Rutsaert, P., Malabayabas, A. J. B., Lampayan, R. M., Radanielson, A. M., & Singleton, G. R. (2016). Yield gaps in rice-based farming systems: Insights from local studies and prospects for future analysis. *Field Crops Research*, *194*, 43–56. https://doi.org/10.1016/j.fcr.2016.04.039

Stutz, D., Hermans, A., & Leibe, B. (2018). Superpixels: An evaluation of the state-of-the-art. *Computer Vision and Image Understanding*, *166*, 1-27.

Tadesse, W., Zegeye, H., Debele, T., Kassa, D., Shiferaw, W., Solomon, T., ... & Assefa, S. (2022). Wheat production and breeding in ethiopia: retrospect and prospects. *Crop Breeding, Genetics and Genomics*, 4(3).10.20900/cbgg20220003.

Tamene, L., Abera, W., Bendito, E., Erkossa, T., Tariku, M., Sewnet, H., Tibebe, D., Sied, J., Feyisa, G., Wondie, M., & Tesfaye, K. (2022). Data-driven similar response units for agricultural technology targeting: An example from Ethiopia. *Experimental Agriculture*, *58*, e27. https://doi.org/10.1017/S0014479722000126

Tesfaye, K., Jaleta, M., Jena, P., & Mutenje, M. (2015). Identifying potential recommendation domains for conservation agriculture in Ethiopia, Kenya, and Malawi. *Environmental management*, *55*(2), 330-346.

Tomasini, C., Emmendorfer, L., Borges, E. N., & Machado, K. (2016). A methodology for selecting the most suitable cluster validation internal indices. *Proceedings of the 31st Annual ACM Symposium on Applied Computing*, 901–903. https://doi.org/10.1145/2851613.2851885

Trabucco, A., & Zomer, R. J. (2018). Global aridity index and potential evapotranspiration (ET0) climate database v2. *CGIAR Consort Spat Inf*, *10*, m9.

van Bussel, L. G. J., Grassini, P., Van Wart, J., Wolf, J., Claessens, L., Yang, H., Boogaard, H., de Groot, H., Saito, K., Cassman, K. G., & van Ittersum, M. K. (2015). From field to atlas: Upscaling of location-specific yield gap estimates. *Field Crops Research*, *177*, 98–108. https://doi.org/10.1016/j.fcr.2015.03.005

Van Ittersum, M. K., Van Bussel, L. G., Wolf, J., Grassini, P., Van Wart, J., Guilpart, N., ... & Cassman, K. G. (2016). Can sub-Saharan Africa feed itself?. *Proceedings of the National Academy of Sciences*, *113*(52), 14964-14969.

van Ittersum, M. K., Cassman, K. G., Grassini, P., Wolf, J., Tittonell, P., & Hochman, Z. (2013). Yield gap analysis with local to global relevance—A review. *Field Crops Research*, *143*, 4–17. https://doi.org/10.1016/j.fcr.2012.09.009

van Wart, J., van Bussel, L. G. J., Wolf, J., Licker, R., Grassini, P., Nelson, A., Boogaard, H., Gerber, J., Mueller, N. D., Claessens, L., van Ittersum, M. K., & Cassman, K. G. (2013). Use of agro-climatic zones to upscale simulated crop yield potential. *Field Crops Research*, *143*, 44–55. https://doi.org/10.1016/j.fcr.2012.11.023

Vanlauwe, B., Tittonell, P., & Mukalama, J. (2007). Within-farm soil fertility gradients affect response of maize to fertiliser application in western Kenya. In A. Bationo, B. Waswa, J. Kihara, & J. Kimetu (Eds.), *Advances in Integrated Soil Fertility Management in sub-Saharan Africa: Challenges and Opportunities* (pp. 121–132). Springer Netherlands. https://doi.org/10.1007/978-1-4020-5760-1_10

Veldkamp, A., Kok, K., De Koning, G. H. J., Schoorl, J. M., Sonneveld, M. P. W., & Verburg, P. H. (2001). Multi-scale system approaches in agronomic research at the landscape level. *Soil and Tillage Research*, *58*(3), 129–140. https://doi.org/10.1016/S0167-1987(00)00163-X

Walhazi, H., Maalej, A., & Amara, N. E. B. (2024). A multi-classifier system for automatic fingerprint classification using transfer learning and majority voting. *Multimedia Tools and Applications*, *83*(2), 6113–6136. https://doi.org/10.1007/s11042-023-15337-6

Wang, S., Azzari, G., & Lobell, D. B. (2019). Crop type mapping without field-level labels: Random forest transfer and unsupervised clustering techniques. *Remote Sensing of Environment*, *222*, 303–317. https://doi.org/10.1016/j.rse.2018.12.026

White, J. W., Tanner, D. G., & Corbett, J. D. (2001). An agro-climatological characterization of bread wheat production areas in Ethiopia.https://doi.org/10.1016/j.agee.2007.06.006

Williams, C. L., Hargrove, W. W., Liebman, M., & James, D. E. (2008). Agro-ecoregionalization of Iowa using multivariate geographical clustering. *Agriculture, Ecosystems & Environment*, *123*(1), 161–174. https://doi.org/10.1016/j.agee.2007.06.006

Wu, F., Wu, B., Zhang, M., Zeng, H., & Tian, F. (2021). Identification of crop type in crowdsourced road view photos with deep convolutional neural network. *Sensors*, *21*(4), 1165.

Xu, Z., Chen, J., Xia, J., Du, P., Zheng, H., & Gan, L. (2018). Multisource earth observation data for land-cover classification using random forest. *IEEE Geoscience and Remote Sensing Letters,* 15(5), 789-793.

Xu, H., Huang, F., Zuo, W., Tian, Y., Zhu, Y., Cao, W., & Zhang, X. (2020). Impacts of spatial zonation schemes on yield potential estimates at the regional scale. *Agronomy*, *10*(5), 631.

Xu, R., & Wunsch, D. (2005). Survey of clustering algorithms. *IEEE Transactions on Neural Networks*, *16*(3), 645–678. https://doi.org/10.1109/TNN.2005.845141

You, L., and Guo, Z. (2024). Spatial Allocation of Agricultural Production: IFPRI's latest SPAM2020.

You, L., Wood, S., & Wood-Sichra, U. (2009). Generating plausible crop distribution maps for Sub-Saharan Africa using a spatially disaggregated data fusion and optimization approach. *Agricultural Systems*, *99*(2-3), 126-140.

You, L., Wood, S., & Wood-Sichra, U. (2009). Generating plausible crop distribution maps for Sub-Saharan Africa using a spatially disaggregated data fusion and optimization approach. *Agricultural Systems*, *99*(2), 126–140. https://doi.org/10.1016/j.agsy.2008.11.003

Zhang, Y., & Hepner, G. F. (2017). The Dynamic-Time-Warping-based k-means++ clustering and its application in phenoregion delineation. *International Journal of Remote Sensing*, *38*(6), 1720–1736. https://doi.org/10.1080/01431161.2017.1286055

Zanaga, D., Van De Kerchove, R., Daems, D., De Keersmaecker, W., Brockmann, C., Kirches, G., Wevers, J., Cartus, O., Santoro, M., Fritz, S., Lesiv, M., Herold, M., Tsendbazar, N.-E., Xu, P., Ramoino, F., & Arino, O. (2022). ESA WorldCover 10 m 2021 v200 (Version v200) [Data set]. Zenodo. https://doi.org/10.5281/zenodo.7254221.